Renewable Energy 189 (2022) 1324–1336

Contents lists available at ScienceDirect

Renewable Energy

journal homepage: www.elsevier.com/locate/renene

# Role of phase change materials in backfilling of flat-panels ground heat exchanger

Michele Bottarelli*, Eleonora Baccega, Silvia Cesari, Giuseppe Emmi

*Department of Architecture, University of Ferrara, Via Quartieri 8, Ferrara, 44121, Italy*

ARTICLE INFO

*Article history:*
Received 4 October 2021
Received in revised form
15 February 2022
Accepted 9 March 2022
Available online 12 March 2022

*Keywords:*
Multi-source heat pumps
Ground heat exchangers
Phase change materials
Experimental test

ABSTRACT

The behaviour of a multi-source heat pump system coupled with phase change materials (PCMs) is discussed in this manuscript, as based on selected data collected during one-year testing at the TekneHub Laboratory of the University of Ferrara (Italy), as a synergic prototype setup of two European projects: IDEAS, an H2020 project, and CLIWAX, an EFDR project. Three geothermal loops of novel shallow Flat-Panels ground heat exchangers (GHX) provide the coupling of a water-to-water heat pump with the ground, as backfilled with sand, a mixture of sand and granules with paraffins and containers filled in with hydrated salts. Furthermore, two hybrid photovoltaic panels and a dry-cooler complete the exploitable thermal sources landscape. Finally, a control unit manages all the elements for the exploitation of the different thermal sources. How the increased underground thermal energy storage is driven by PCMs has been investigated by means of specific tests, and compared with the standard case of backfilling sand. Results confirm that PCMs can compensate peak loads occurring during hard weather conditions. Good performances of the multi-source heat pump were found, with a winter coefficient of performance always higher than 5. Finally, the application of PCM in summer should be preferred in climatic zones with hot summers and cold winters, With evidence, latent heat, thermal conductivity and melting point of PCMs should be tuned accordingly to the energy requirements and the local ground thermal conditions.



## 1. Introduction

Multi-source heat pump systems (MSHPs) are designed to switch between mutual and complementary thermal sources, to select more profitable temperatures, reduce frosting issues and therefore increase the overall performance. In the building footprint, the most widespread thermal sources are air, sun and soil. However, ground is the unique source that allows to store thermal energy and it provides more favourable and stable temperatures than outdoor air temperatures [1,2]. One of the ways of harvesting geothermal energy is represented by ground heat exchangers (GHXs) coupled with a heat pump (HP), thus involving additional costs that may be quite important depending on GHXs typology [3,4]. GHXs can be installed in vertical boreholes or in shallow horizontal diggings, also referred as VGHXs and HGHXs respectively [5]. The former enables to rely on stable temperatures in the deep soil beyond 20 m [6,7], but require high costs for drilling and installation procedure [8], thus ultimately reducing the economic feasibility of the project [9]. Furthermore, at higher depth (80–120 m) their performance can be negatively impacted by soil thermal imbalance caused by heat extraction. In addition, the low ground thermal conductivity results in lowering the temperature of the soil in a small number of years [10]. Differently from VGHXs, HGHXs are installed at a depth of only 2–3 m, therefore their performance is affected by the variations of climatic conditions [11]. However, this technology does not suffer thermal imbalance issues when adopted in mild climate [12]. One of the main benefits related to HGHXs is represented by the considerably easier installation procedure compared to VGHXs. HGHXs require the excavation of a shallow trench and the dug ground can be directly employed as backfilling material. Moreover, the installation layout is characterised by higher flexibility [13], and geologic requirements are not so strict as for VGHXs thanks to the limited depth [12,14]. Nevertheless, HGHXs hold some drawbacks. Indeed, the lower thermal performance caused by seasonal variations in ground temperature requires decisively higher soil surfaces [14,15]. Furthermore, payback time still remains too long to justify the initial investment,

* Corresponding author.
*E-mail address:* michele.bottarelli@unife.it (M. Bottarelli).

https://doi.org/10.1016/j.renene.2022.03.061

although installation costs are lower than for VGHXs [16].

Towards a reduction in the size and costs of the ground coupling, recent research efforts have attempted to develop more efficient HGHXs, such as the novel Flat-Panel developed at the University of Ferrara in 2012 [11,16,17]. Moreover, the thermal behaviour of a HGHE is highly dependent on the thermal properties of backfilling materials and the surrounding soil [18]. Ideal backfilling materials are beneficial for the reduction of total thermal resistance and the improvement of the heat exchange performance of the HGHX [19,20]. Considering thermal conductivity, sand ensures high values of it, equal to about 1.3 W/(m·K), and it results to be the least expensive backfilling material at the same time [6]. However, with the aim of increasing the thermal performance of HGHXs, also the thermal storage capacity of backfilling materials must be enhanced.

Against this background, phase change materials (PCMs) result to be suitable candidates. During the phase change process, they can store or release energy in the form of latent heat in a ratio of 5–14 times higher than sensible thermal energy storage materials, thus allowing to reduce the size of plants and therefore their costs [21,22]. Based on the nature of chemical composition, PCMs are divided into organic, inorganic and eutectic materials, which can be a combination of organic-organic, organic-inorganic and inorganic-inorganic components. Considering the application to GHXs backfilling material, organic PCMs, and especially paraffins, should be adopted due to their significant latent heat [23–25]. Moreover, paraffins are non-corrosive, non-toxic and environmentally friendly. They benefit from no phase segregation, low degree of supercooling and a considerable reliability during transition cycles, along with chemical stability [26,27]. On the other hand, they present an extremely low thermal conductivity, usually between 0.1 and 0.3 W/(m·K) [28,29], which can reduce the efficiency of GHX and possibly prevent PCM from completing the phase change. Differently, inorganic PCMs like hydrated salts are characterised by a higher thermal conductivity than organic compounds, ranging from 0.6 to 1 W/(m·K) [30], and by a lower cost. However, they present the tendency to undergo phase segregation, chemical instability, and low thermal stability. In addition, due to their corrosive behaviour, inorganic PCMs must be macro-encapsulated in plastic containers [31].

Except for the numerical investigation carried out by Rabin and Korin in 1996 [32], the use of PCMs as additive to backfilling material for the GHX has started to be investigated only in the last decade, therefore the topic is still a recent field of study. A list of the works focused on this application is reported in Table 1. Research has been almost exclusively conducted by numerical analysis, uncovering a lack of experimental investigations [19] and thus generating a critical knowledge gap about the realistic behaviour of the system.

As already mentioned above, Rabin and Korin [32] were the first to study the integration of PCMs mixed with sand as backfilling material for the GHX. Results of the numerical analysis, which considered organic PCMs and VGHXs, demonstrated that PCM backfilling is able to increase the thermal performance of the system. Only more than ten years later, Lei and Zhu [33] compared the application of paraffin with the use of a binary mixture of capric acid (CA) and lauric acid (LA). Similarly, Qi et al. [25] investigated the adoption of paraffin, a mixture of CA and LA, and the same mixture with metal particles for thermal conductivity enhancement. Findings showed that higher heat transfer performance can be obtained by using enhanced PCM. Again, a few other works focused on the adoption of acid mixtures [23,34], sometimes compared with paraffin [35] or only on the use of paraffin [36,37]. Whilst the studies mentioned above are based only on organic PCMs, Zhang et al. [38] investigated the thermal performance of a single U-tube borehole heat exchanger (BHE) backfilled with hydrated salts. Numerical results showed that the temperature differences of the working fluid at the inlet and outlet after 6 h of cooling operation increased compared to the corresponding temperature differences in the BHE containing a conventional backfill.

Despite the limited number of works on the topic, the review of the literature as reported in Table 1 uncovers that even less studies have been focused on the integration of PCMs in the backfilling material for HGHXs. Thermal performance of soil backfilling for HGHX with micro-encapsulated paraffin was numerically investigated by Dehdezi et al. [39]. Results demonstrated that PCM-modified soil increased the coefficient of performance (COP) of a heat pump system by 17% compared with ordinary soil backfilling. Bottarelli et al. investigated the adoption of paraffin-based granules [40] and of micro-encapsulated paraffin [41] mixed with the backfilling soil (sand) of the novel Flat-Panel HGHX mentioned in Ref. [17]. Results of the numerical analysis showed that the application of PCMs allows to mitigate variations in ground temperature caused by seasonality and heat pump action, also ensuring a higher COP. Moreover, the depletion of the latent heat due to the PCMs solidification/melting could be recharged during the summer/winter season, which therefore achieves the seasonal ground thermal storage.

To sum up, research findings show that the application of PCMs as additive to GHXs backfilling material is significantly advantageous, especially for HGHXs [41]. This technology mitigates ground temperature variations, thus improving the thermal performance of the system without high installation costs. Indeed, differently from common thermal storage tanks, which requires dedicated technical spaces, the adoption of PCMs mixed in HGHXs backfilling material does not occupy any precious building volume and its realisation can be carried out during HGHXs excavations without additional costs due to additional tanks or to more GHXs installations. Finally, considering PCM recovery and disposal at the end-of-life, these procedures would be easier for HGHEs compared to VGHXs.

Nevertheless, review of the literature reported above has uncovered that only numerical studies have been conducted and nearly all of them focused on VGHXs. Furthermore, all the works exclusively investigated

The application of organic PCMs, even though inorganic PCMs like hydrated salts present several advantages. Therefore, current literature suffers from a lack of experimental data and validation about the integration of PCMs in backfilling material for HGHXs, as well as of experimental investigation comparing the performance of the system when organic and inorganic PCMs like hydrated salts are adopted.

Addressing these remarks, preliminary results are here reported and discussed about the large-scale experimental investigation of HGHXs with three different backfilling materials: sand, a mixture of sand with paraffin-based granules and macro-encapsulated hydrated salts. Data have been collected during one-year testing of a MSHP prototype system (Fig. 1) operating since summer 2020 at the TekneHub Laboratory of the University of Ferrara (Italy), as synergic setup for two European projects: IDEAS [42], an H2020 project, and CLIWAX [43], an EFDR project.

## 2. Setup description

The setup is a multisource water-to-water HP system devoted to the air-conditioning of a small mock up (40 $m^3$). The vertical envelope is composed of 12 cm thick insulation panels, while horizontal elements are represented by a concrete slab with a PCM integrated radiant floor and a 3 cm thick wooden roof with 3 cm of gravel laid above.

**Table 1**
Studies about the integration of PCMs in GHX backfilling material (num = numerical, exp = experimental, H = horizontal, V = vertical, O = organic, I = inorganic, E = eutectic).

| Ref. | Year | Study | GHX | PCM | Melting temperature | Scenarios | Period analysed |
|---|---|---|---|---|---|---|---|
| [32] | 1996 | num | V | O - paraffin<br>O - GPCM[a] | from 44 to 46 °C | • without PCM<br>• paraffin<br>• GPCM | year |
| [33] | 2009 | num | V | O - paraffin<br>O - CA-LA (66:34) | 5.5 °C<br>25.4 °C | • without PCM<br>• with PCM | winter and summer |
| [39] | 2011 | num | H | O - paraffin | 26 °C | • without PCM<br>• 10% PCM-modified soil<br>• 20% PCM-modified soil<br>• 40% PCM-modified soil<br>• 60% PCM-modified soil<br>• 80% PCM-modified soil | 01/07/1996 to 01/10/1996 |
| [36] | 2013 | num | V | O - paraffin | – | – | – |
| [37] | 2014 | num | V | – | – | • without PCM<br>• ordinary PCM<br>• enhanced PCM | – |
| [40] | 2015 | num | H | O - paraffin-based granules for winter (65%)<br>O - paraffin-based granules for summer (35%) | 4 °C<br>26 °C | • without PCM<br>• with PCM | year |
| [41] | 2015 | num | H | O - paraffin | 26 °C | • without PCM<br>• with PCM | year |
| [25] | 2016 | num | V | O - paraffin RT27<br>O - CA-LA (66:34)<br>E – CA-LA with metal particles | 28–30 °C<br>20.4 °C<br>20.4 °C | • without PCM<br>• ordinary PCM<br>• enhanced PCM | summer |
| [34] | 2016 | num | V | E – CA-LA with 10% of silica and 6% of expanded graphite + organic compounds (40% LA - 60% CA) | 20 °C | • without PCM<br>• SSPCM[b] | |
| [35] | 2018 | num | V | O - paraffin<br>O - CA-LA based SSPCM | 25 ± 2 °C<br>19.9 °C | • without PCM<br>• paraffin<br>• SSPCM | 5 days |
| [38] | 2019 | num | V | I - hydrated salts | 23 °C | • without PCM<br>• with PCM | 24h |
| [23] | 2019 | lab-scale exp/num | V | O - oleic acid for winter<br>O - decyl acid-LA (66:34) for summer | 8.1 °C<br>20.5 °C | • without PCM<br>• with PCM | winter and summer |

[a] PCM elements containing a material that has the same thermophysical properties as those of the soil, but latent heat and phase transition temperatures as of paraffin.
[b] Shape-stabilised PCM.

At the source-side, coupled with the HP, the setup consists of three main thermal sections exploiting ground, sun and air, respectively. The geothermal section operates with three geothermal loops, 6 m long each, of novel Flat-Panels GHXs, and the scheme of the trenches' section is reported in Fig. 2. The GHXs provide the coupling of the ground with a water-to-water HP (6 kW), as backfilled with sand (GHX1), a mixture of sand and granules with paraffins (GHX2) and cylindrical high-density polyethylene (HDPE) containers filled in with hydrated salts (GHX3). In Fig. 3 are depicted the backfilling material of sand mixed with granules as well as the HDPE containers. Both paraffins and HDPE containers with PCMs were provided by PCM Products Ltd [44], partner of IDEAS project. As reported in Tables 2–4, where the main thermophysical properties of the different backfilling materials are summarised, the latent heat improving GHX2 is 15 kWh of which 8.7 kWh with a melting point of 8 °C and 6.3 kWh of 27 °C; similarly for GHX3. All the trenches were also filled in with water to increase the thermal conductivity and the heat capacity of the backfilling material.

The solar section is composed of two hybrid photovoltaic panels (PVT), coupled with a tank (200 l) in which about 150 kg of PCMs filling n.76 cylindrical high-density polyethylene (HDPE) containers are installed, of which n.59 with a melting point of 10 °C and n.17 of 32 °C. Also in this case, macro-encapsulated PCMs were provided by PCM Products Ltd. Finally, a dry-cooler completes the thermal sources landscape, as a way to exploit air. This exchanger was voluntarily undersized to minimise the power demand of the fan and therefore to limit the operating in overheating conditions of PVT panels and GHXs. A control unit manages all the devices and several proportional valves, which set the hydronic loop for the exploitation of the different sources. A specific algorithm for the optimisation of the system has been developed and currently still under revision.

At user-side, a radiant floor, in which n.75 HDPE containers filled in with PCMs are installed, provides the air-conditioning of a full monitored room. Two different melting points were selected: n.50 containers were filled with a PCM with a melting temperature of 21 °C (cooling period), and n.25 with 27 °C (heating period). In Fig. 4 a picture of the small-scale set-up is depicted.

## 3. Monitoring system

Several probes were placed in correspondence of each thermal section to constantly monitor the thermodynamic state of all the components of the system. Values regarding temperature, heat flux, mass flow rate, thermal and electrical power were continuously read at regular time steps. 4-wires RTDs with metal tip [45] were installed on the hydraulic loop at the inlet and outlet of each thermal section (ground, sun, air), on each buffer tank (source side, user side and on the PVT loop) and in correspondence of the outlet of each geothermal loop. T-type thermocouples [46] were installed on top of each PVT panel and in between the layers of the radiant

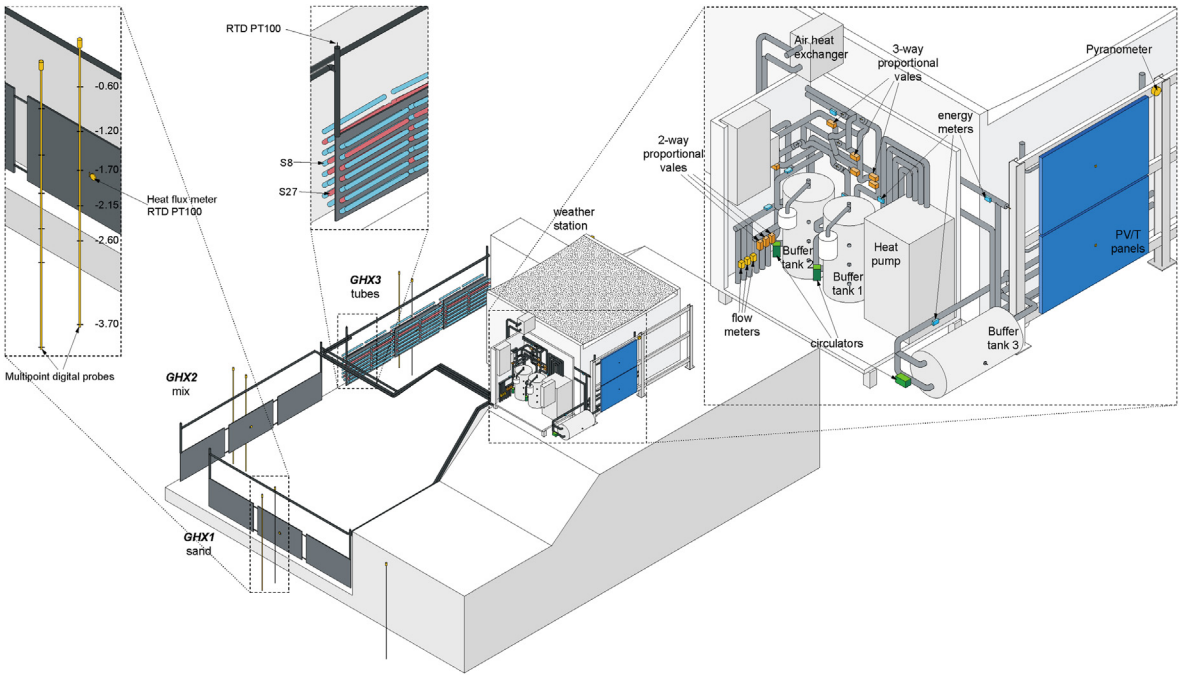


**Fig. 1.** Sketch of the system set-up.

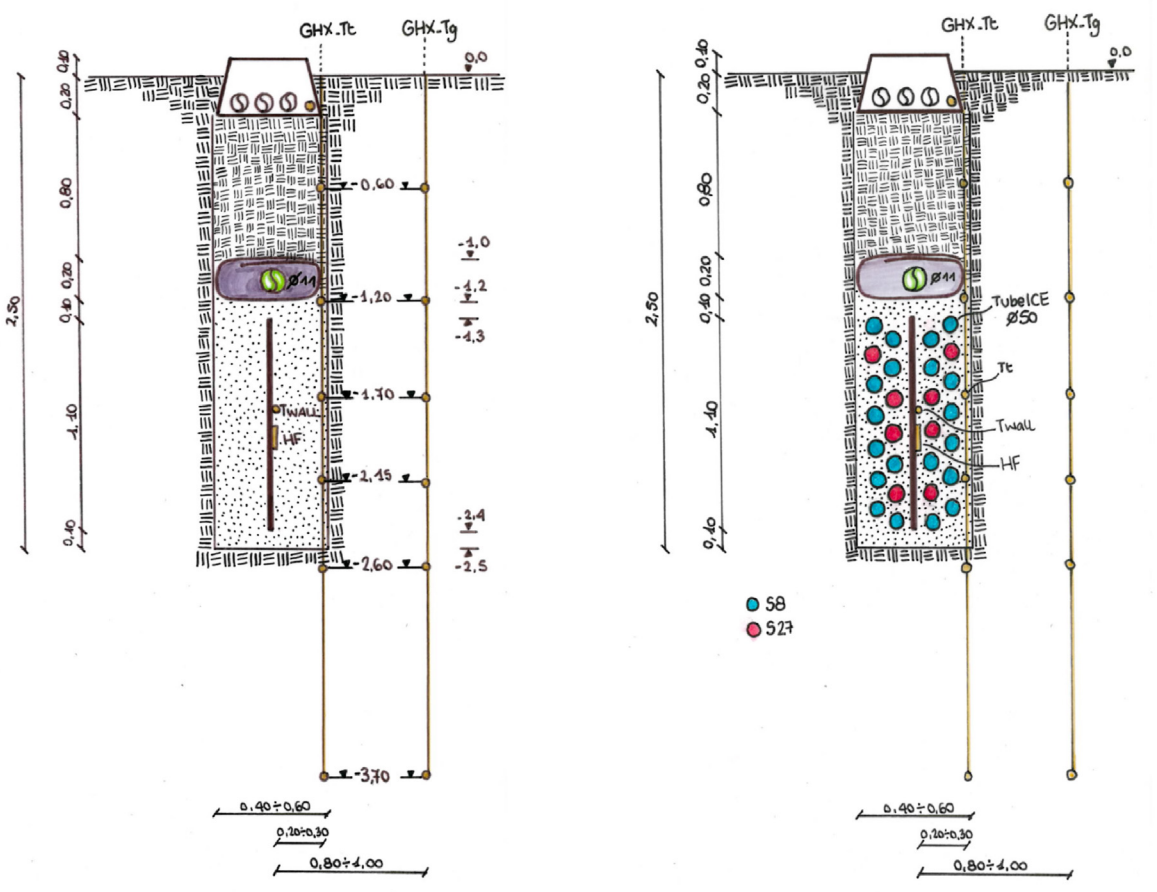


**Fig. 2.** GHXs arrangements into trenches: GHX1 and GHX2 on the left (sand, sand & granules), GHX3 on the right (tubes).

**Fig. 3.** Sand mixed with granules and tubes arrangement.

**Table 2**
GHX1 trench backfilling material (sand).

| | Heating | Cooling | Unit |
|---|---|---|---|
| Dry sand | 8.3 | 8.3 | t |
| Water | 2.5 | 2.5 | t |
| Wet sand UTES (10K) | 171.0 | 171.0 | MJ |

**Table 3**
GHX2 trench backfilling material (granules).

| | Heating | Cooling | Unit |
|---|---|---|---|
| Dry sand | 6.1 | 6.1 | t |
| Water | 1.8 | 1.8 | t |
| Wet sand UTES (10K) | 126.5 | 126.5 | MJ |
| Melting point | 8 | 27 | °C |
| PCM type | A8 | A27 | |
| Specific heat | 2.16 | 2.22 | kJ/(kg·K) |
| Latent heat | 180 | 250 | kJ/kg |
| PCM mass | 174 | 89 | kg |
| Product mass | 348 | 178 | kg |
| PCM STES | 3.8 | 2.0 | MJ |
| PCM LTES | 31.3 | 22.2 | MJ |

**Table 4**
GHX3 trench backfilling material (tubes).

| | Heating | Cooling | Unit |
|---|---|---|---|
| Dry sand | 7.6 | 7.6 | t |
| Water | 2.3 | 2.3 | t |
| Wet sand UTES (10K) | 156.5 | 156.5 | MJ |
| Melting point | 8 | 27 | °C |
| PCM type | S8 | S27 | |
| Specific heat | 1.9 | 2.2 | kJ/(kg·K) |
| Latent heat | 130 | 185 | kJ/kg |
| PCM mass | 241 | 120 | kg |
| Number of containers | 112 | 56 | |
| PCM STES | 4.6 | 2.6 | MJ |
| PCM LTES | 31.3 | 22.2 | MJ |

floor, i.e., on top of the concrete mortar, on the HDPE containers, on the floor surface. Multi-point digital TT probes [47] were installed into the soil to read temperatures at different depths. More specifically, two probes were used for each geothermal loop, one 0.20 m and the other one 1 m far from the central panel, plus an additional one in the undisturbed soil. The sensors in each probe were arranged at 0.60 m, 1.20 m, 1.70 m, 2.15 m, 2.60 m, and 3.70 m deep from the ground surface. Heat flux meters [48] were installed on the central panel of each geothermal loop and in different positions of the radiant floor, based on the arrangement of the HDPE containers. Flow meters [49] were used at the inlet of each geothermal loop to ensure the same mass flow rate. All the above-mentioned sensors were connected to a datalogger [50] that collected data at regular and customisable time steps, that was 1 min. The monitoring system was also equipped with thermal energy meters [51] which were installed at the inlet and/or outlet of each component or device and gathered values about the instant and total mass flow rate, the instant and total power, the seasonal progressive energy consumptions and the inlet and outlet temperatures. These twelve devices were connected to a Mbus gateway [52] and data were continuously collected at regular and customisable time steps, that was 5 min at the beginning of the monitoring activity but that was reduced to 1 min for the winter season. To complete the whole system, a weather station and a pyranometer were installed to monitor the boundary conditions [53,54]. In Table 5 the accuracy of the sensors used in the monitoring campaign are reported and in Fig. 5 the scheme of the source side system layout with sensors' position is represented.

## 4. Results

As described in the previous sections of the paper, the main objective of this research is the study of the thermal behaviour of the enhanced ground heat source for HP applications, from both qualitative and quantitative point of view. For this purpose, several key variables and parameters have been measured and logged during the system operation in summer and winter, respectively. On the source side, the supply and return temperatures from each loop, geothermal, air and solar, together with the volume flow rates have been monitored in order to have a wide overview of the behaviour of the system and to evaluate the heat fluxes involved in the system.

Outlet temperatures of each geothermal loop, together with air temperature, collected during four summer days are reported in Fig. 6, which can be read on the basis of the following considerations. The temperature peaks stand for the switching on of the HP,

**Fig. 4.** View of the small-scale set-up.

**Table 5**
Accuracy of the sensors used.

| Sensor | Accuracy |
|---|---|
| RTD PT100 [35] | 0.15 K |
| T-type thermocouple [36] | 0.5 K |
| Multipoint probes [37] | 0.5 K |
| Heat flux meter [38] | 5% at 23 °C |
| Flow meter [39] | 6% of the measured value (20%–100%)<br>1.2% of full scale (0%–20%) |
| Energy meter [41] | <5% for the flow meter<br>0.5 K for temperature |
| Pyranometer [44] | <1% (between 10 °C and 40 °C) |

whose frequency during the day is higher than during the night. This is obviously due to the very low cooling demand at night and the outlet temperatures which were almost identical to the one set in the indoor environment. The thermal behaviour of the different GHXs is the focus of the chart in which, in particular, it is interesting to notice that during the hottest hours of each day the continuous switching on/off of the HP brought to differences between the three geothermal loops. As it can be seen by the different colours of the curves, the temperature trends are characterised by an offset to each other. By the end of each day, the outlet temperature of GHX1 was slightly higher than GHX2 and up to 0.5 K higher than GHX3.

Similar considerations can be done for the winter period, where the behaviour of four consecutive days is illustrated in Fig. 7. In this case, the HP was continuously switching on/off and in two days (11–13 February) the outlet temperature of GHX1, initially equal to the other loops, decreased faster and differences reached about 0.5 K.

The monitoring activity started in August 2020, but at the beginning there was no control system as the first algorithm was implemented in September 2020. At the beginning of the monitoring activity, several systems layouts were analysed activating each of the three GHXs individually. In Fig. 7 the behaviour of a summer day with no control rules during which only the geothermal loop, more specifically only GHX2, was activated, is reported in terms of outdoor air temperature (OUT_T), source side buffer tank temperature (BF1_T), which represents the supply temperature to the GHXs, outlet temperature for GHX2 (GHX2_Tout) and energy stored and released in GHX2 (GHX2_HF+ and GHX_HF-, respectively). On the right y-axis, the red dotted line stands for the energy absorbed by the ground and the blue dotted one for the energy released by the ground. Since there was no control algorithm, the system was manually set in ground mode as during the day it was the most convenient source to draw from. In fact, as soon as the air temperature increased forcing the HP to turn on, the energy stored in the ground started to grow, and after 12 h of operation, the amount of heat stored was about 250 Wh/m$^2$ (this value is referred to just one side of the Flat-Panels, so the value per meter of trench would be of 500 Wh/m$^2$).

After the first control rules started managing part of the system, the effect of the interaction between the different sources is clearly visible.

For instance, the behaviour of a summer day with the control system working is depicted in Fig. 8. The system was set with ground as source for the HP, and air was used as the means with which regenerate the ground by dissipating the stored heat. As the air temperature increased and the HP turned on, the energy stored in the ground started to grow, as the outlet temperature of GHX2 did. Once the outlet temperature of GHX2 became higher than the air temperature, the AHX was turned on to lower the temperature of water returning in BF1. Then, thanks to the sensible decreasing of the air temperature in the late afternoon, a temperature in the buffer tank lower than the GHX2 outlet one was achieved making it possible to extract part of the absorbed heat from the ground. Focusing on 24 h of the system functioning (Fig. 9, September 15th), the energy stored in the ground is of about 450 Wh/m$^2$ (per side of Flat-Panel), while the energy extracted was of about 300 Wh/m$^2$ (per side of Flat-Panel). Moreover, the interaction between these two sources brought to a greater difference between the maximum and minimum temperatures in the buffer tank, and therefore of the leaving temperature in GHX2. In both the days (Figs. 9–10) the difference between the maximum and the minimum air temperature was of about 13 K, but when there was no control algorithm, the temperature in BF1 had a maximum difference of 7 K, while in case of the control algorithm the difference almost doubled and reached nearly 13 K.

During the summer, the control system coupled ground with air in order to extract from the soil during the night part of the heat absorbed during the day. In winter, the ground was coupled with the PVT loop in order to regenerate the soil by exploiting the high

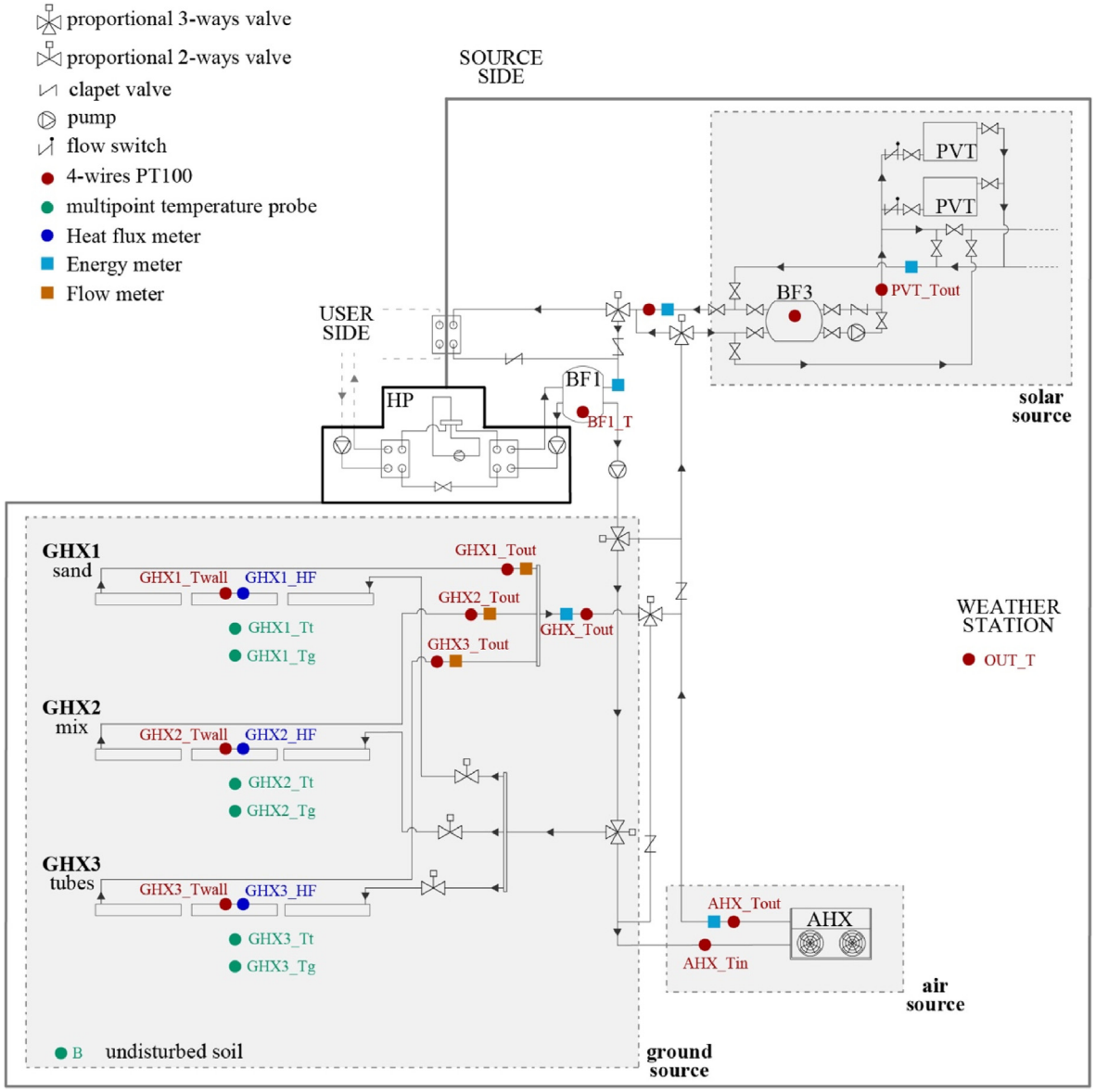


**Fig. 5.** Layout of the source side system and sensors' position.

solar radiation of sunny days. In Fig. 12 a period of three consecutive winter sunny days is illustrated in terms of air temperature, outlet temperatures of the ground and the PVT loops, buffer tank temperature and GHX energy stored and released. This last one is reported on the right y-axis, where the green line stands for the energy absorbed by the soil while the red one for the extracted one. The benefits of the solar recharge are clearly visible as during the central and hottest hours of the day the outlet temperature from the PVT loop, much higher than that of the GHX loop, managed to increase the temperature of the working fluid bringing it from 5 °C to 7–8 °C. The recharge is evident if looking at the energy, where in correspondence of the opening of the PVT loop (central hours of each day) a consistent amount of energy is stored in the ground. Considering the period of three days depicted in Fig. 12, the energy extracted from the ground was of about 550 Wh/m$^2$ (per side of Flat-Panel), while the stored one was of 200 Wh/m$^2$ (per side of Flat-Panel), with therefore an energy balance of 350 Wh/m$^2$ extracted from the ground.

## 5. Discussion

The differences and the effects described in the previous section are better depicted in Fig. 11. As it can be easily seen in the chart, the outlet temperatures of GHX2 and GHX3 (on the y-axis) were compared with those of GHX1 (on the x-axis), which represents the reference case without the enhancement of the ground source. In summer, with outdoor temperature ranging between 27 °C and 32 °C, temperatures obtained from the GHX2 and GHX3 loops were almost always lower than GHX1, with greater differences on the higher temperatures which, according to the Differential Scanning Calorimetry (DSC) curves of the PCMs, correspond to the peak of the latent heat capacity.

Differently, the comparison between the outlet temperature of GHX1 and those of GHX2 and GHX3 during the heating period is reported in Fig. 12. The chart highlights that the temperature in GHX1 is almost always slightly lower and that the greatest differences are visible between 5 °C and 6 °C.

In general, the effect of the PCMs seems visible, even though the

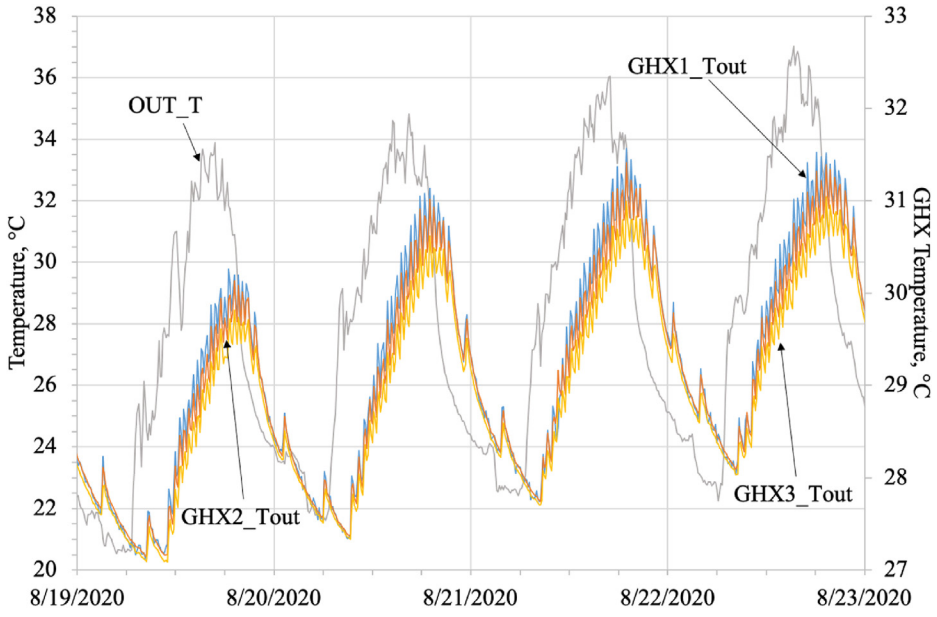


**Fig. 6.** Summer behaviour of GHXs.

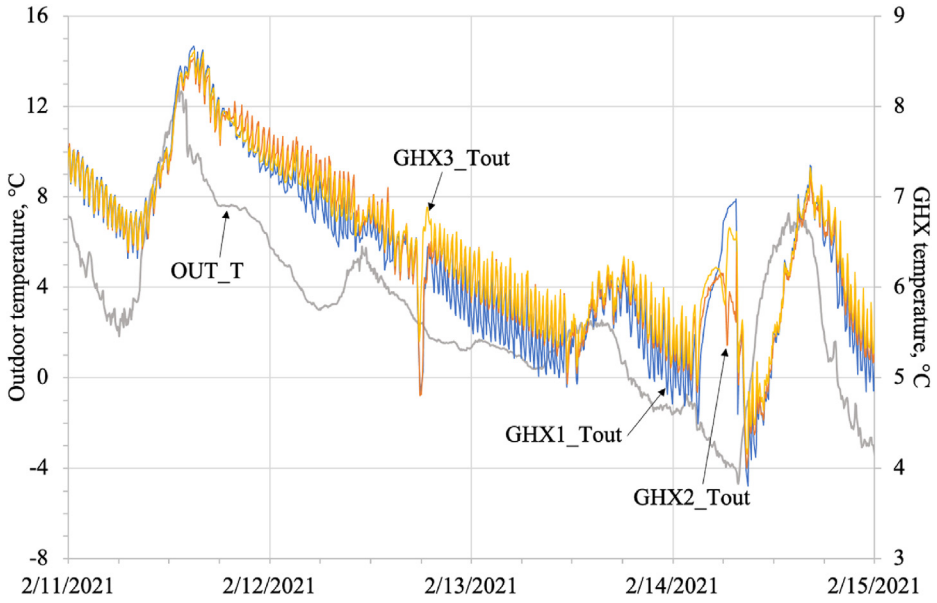


**Fig. 7.** Winter behaviour of GHXs.

enhancement is quite limited. First of all, even though the three loops are overestimated for the system, the length of each one is only 6 m, and this inevitably leads to limited differences between inlet and outlet temperatures, which are normally lower than 1.5 K. Secondly, the three loops work in parallel but converge on the same buffer tank. Therefore, there is a continuous compensation that attenuates the differences between them. Basically, in this configuration the GHX3 and GHX2 are most exploited in this sequence if compared to the exploitation of GHX1. Lastly, the amount of PCM arranged in each trench was limited to keep the costs down but this resulted in a reduced latent heat capacity.

As mentioned before, the control system was subject to continuous revisions and improvements. An extended version of the algorithm which could operate between all the states (each source and their combinations) was implemented during winter. The state frequencies monitored in the period January–March 2021, corresponding to 173.5 h of functioning, are reported in Fig. 13. As expected, given the season, ground was the most

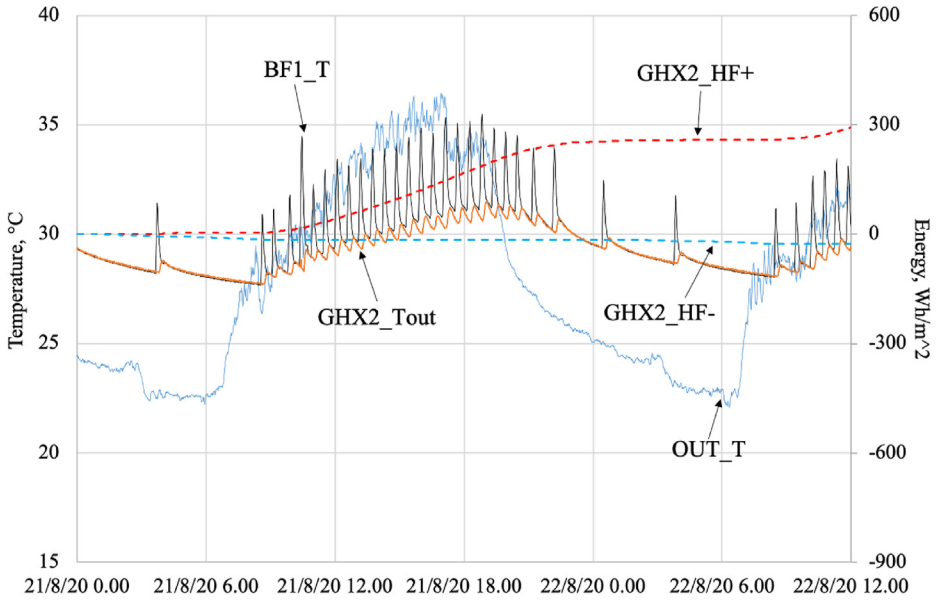


**Fig. 8.** GHX2 behaviour in a summer day without AHX regeneration.

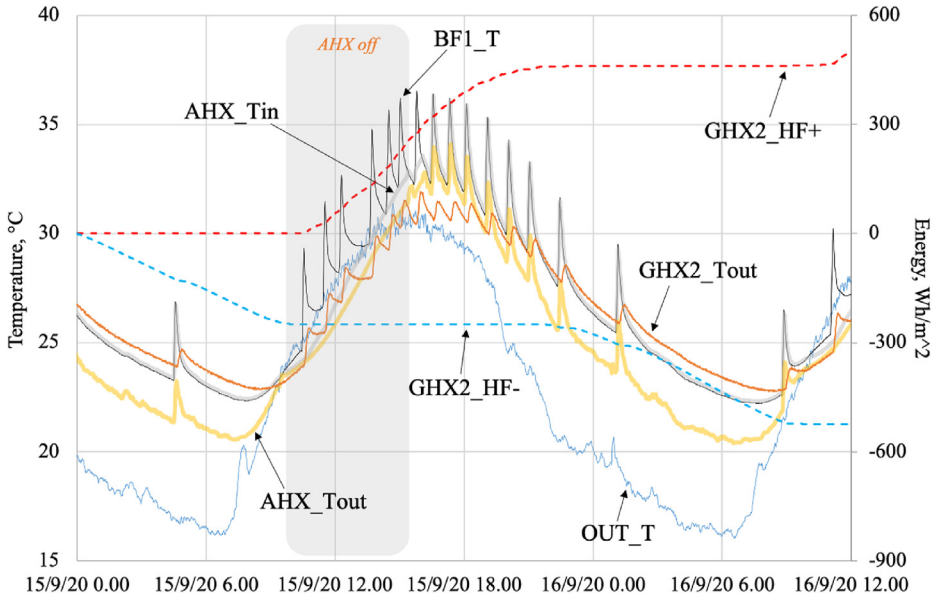


**Fig. 9.** GHX2 behaviour in a summer day with AHX regeneration.

exploited source, which was used as single source for nearly 74% of the time, 16% was coupled with sun and 4% with air. The three sources were exploited together only for 1.1% of the time, so less than 2 h. In general, ground was used for nearly 165 h.

Finally, for the same period (January–March 2021) the COP of each state was calculated. In Fig. 14 the calculated COP for each operating state is depicted. For every source, or every combination of them, the value is always higher than 5, with values higher than 5.5 when the system was operating with air only (COP 5.5), with ground only (COP 5.66), with all the sources together (COP 5.86) reaching the highest value of 6.44 when operating with ground and air.

In general, the values obtained denote good response and performance of the ground and of the system respectively. The increase of 2–3 °C in the evaporation temperature usually corresponds to a reduction of about 10–15% in electricity demand from the HP for the same heating load. In our case, in heating mode, as already highlighted before, the amount of PCM is limited. However, the main results of the research show how it should be possible to increase the energy performance of the HP system with this type of application.

## 6. Conclusions

Results confirm that PCMs mixed into the backfilling of ground heat exchangers can affect the heat transfer by attenuating the

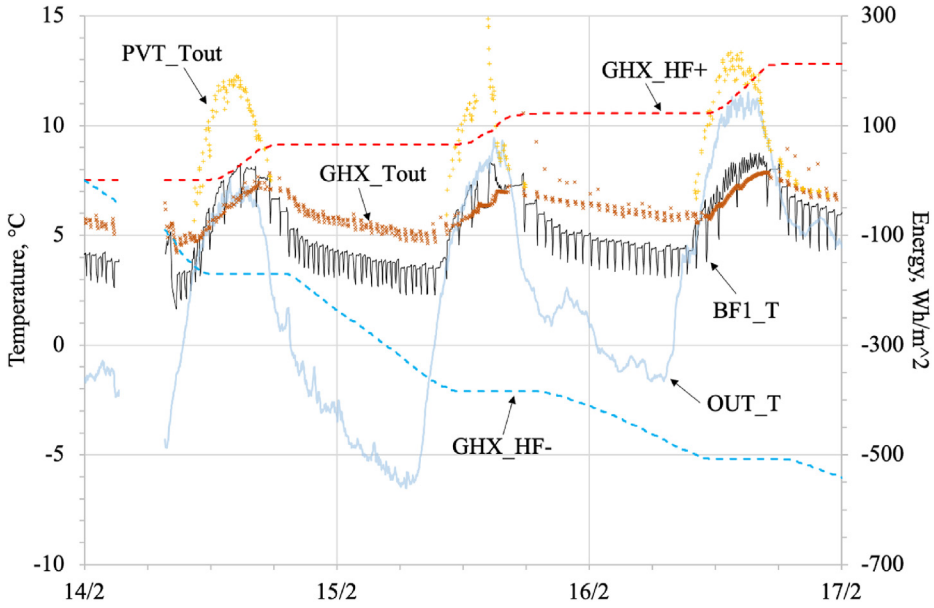


**Fig. 10.** Overall GHX loop temperature in winter season with solar regeneration.

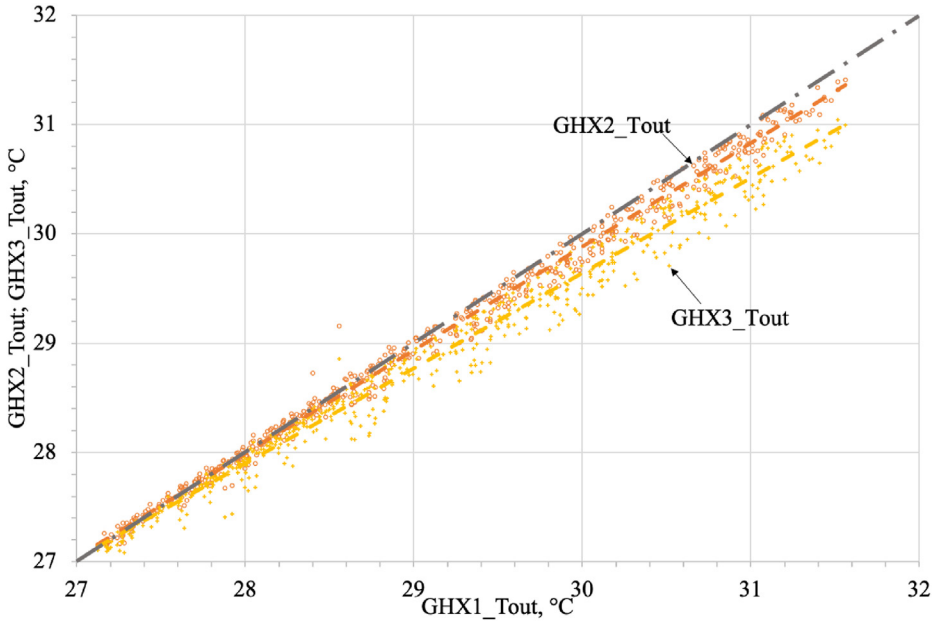


**Fig. 11.** Outlet temperatures from PCM backfilled GHXs vs. sand GHX (19–22 August 2020).

highest temperatures in summer and the lowest in winter. Due to cost restrictions, however, the amount of PCM in each trench is limited and so is the latent heat capacity.

On the basis of what was observed during this one-year monitoring and the cost of PCM, it appears that in climatic zones with hot summers and cold winters, the application of PCM in summer should be preferred rather than the winter one, as water seems to be as suitable as PCM for low temperatures. However, additional considerations should be done for further real scale applications. Firstly, the decision between paraffin and hydrated salts: more stable but more expensive and with lower thermal conductivity the former, with higher volumetric storage capacity but phase segregation and subcooling problems the latter. Secondly, the compatibility of granules (used in GHX2) has not been deeply studied yet.

The collected data also showed good performances of the multi-source heat pump which, being able to exploit three different thermal sources at the same time or in different combinations, had winter COP always higher than 5.

As the ground source was the main focus of this paper, the effect of its regeneration in summer by means of air and its recharge in

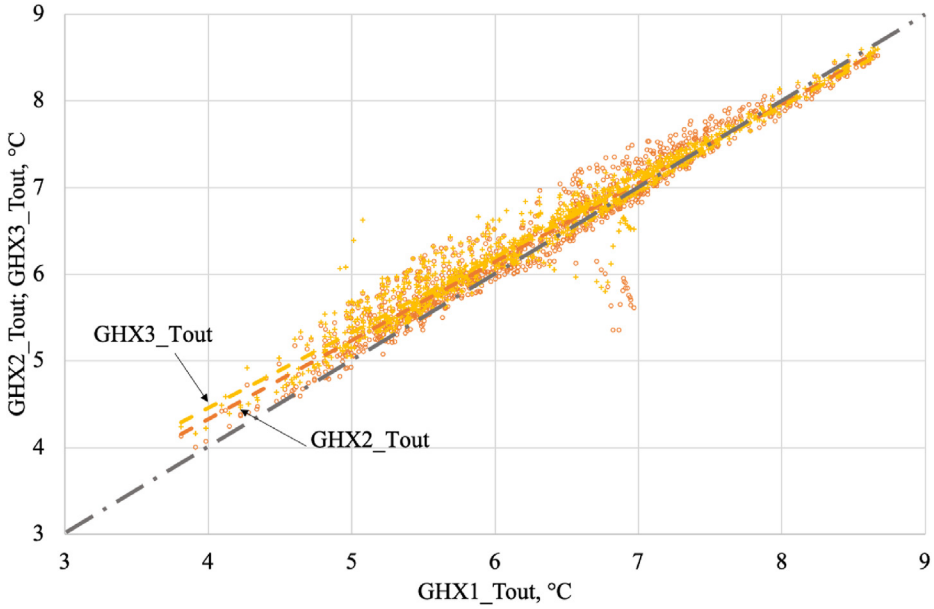


**Fig. 12.** Outlet temperatures from PCM backfilled GHXs vs. sand GHX (11–14 February 2021).

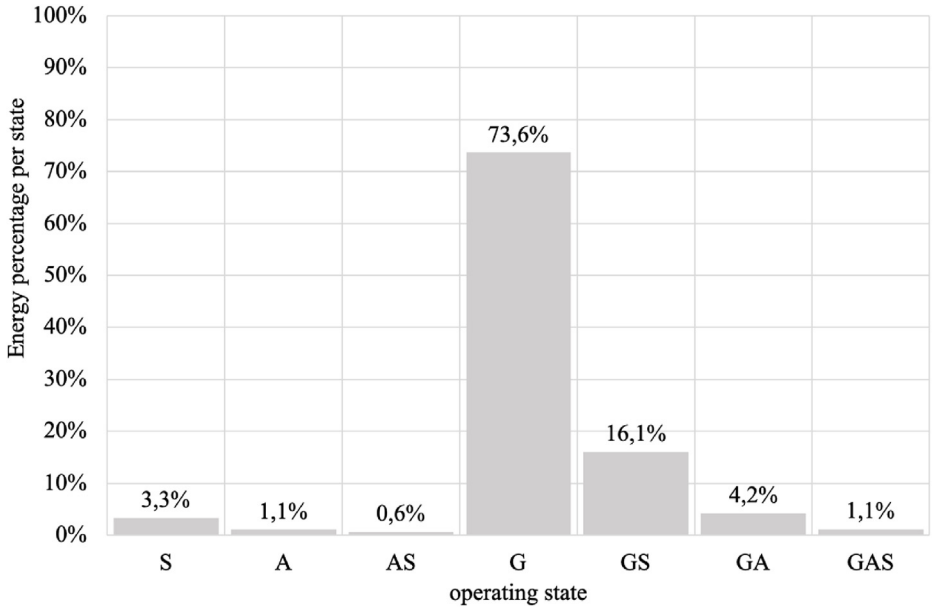


**Fig. 13.** Operating states frequency in winter (G stands for ground, A for air and S for sun).

winter by means of sun were highlighted. However, the effect of the PCM seemed to be quite limited. The reasons are to be found in the total length of each loop, which is only 6 m, the limited amount of material per trench to keep the costs down, the installation of the loops which converge into the same buffer tank and, lastly, the thermal properties of the PCM, especially the granules, that are characterised by low thermal conductivity. On the basis of this last consideration, further developments of the research might involve the improvement of the PCM thermal properties to investigate whether enhanced-PCM might bring to further improvements.

## Declaration of competing interest

The authors declare that they have no known competing financial interests or personal relationships that could have appeared to influence the work reported in this paper.

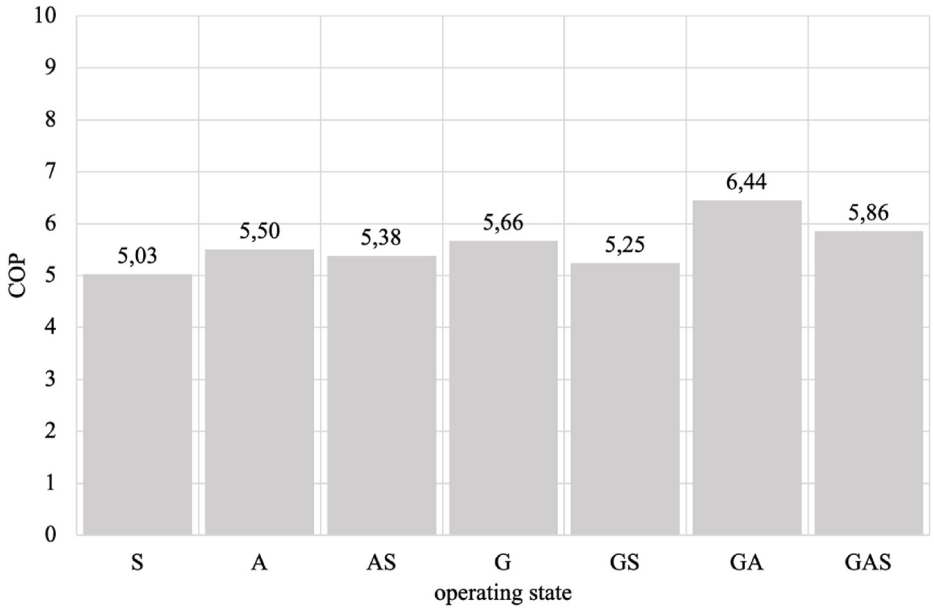


**Fig. 14.** COP of the operating states in winter.

## Acknowledgements

This work was supported financially within the IDEAS project Novel building Integration Designs for increased Efficiencies in Advanced Climatically Tunable Renewable Energy Systems, funded by the European Union's Horizon 2020 research and innovation programme under grant agreement No. 815271. Furthermore, the work was supported within the CLIWAX project, funded by the ERDF programme of the Region Emilia-Romagna (Italy) under grant agreement No. F71F18000160009.

## References

[1] I. Al-Hinti, A. Al-Muhtady, W. Al-Kouz, Measurement and modelling of the ground temperature profile in Zarqa, Jordan for geothermal heat pump applications, Appl. Therm. Eng. 123 (2017) 131–137.
[2] P.D. Pouloupatis, G. Florides, S. Tassou, Measurements of ground temperatures in Cyprus for ground thermal applications, Renew. Energy 36 (2011) 804–814.
[3] H. Javadi, S.S. Mousavi Ajarostaghi, M.A. Rosen, M. Pourfallah, Performance of ground heat exchangers: a comprehensive review of recent advances, Energy 178 (2019) 207–233.
[4] P. Vocale, G.L. Morini, M. Spiga, Influence of outdoor air conditions on the air source heat pumps performance, Energy Proc. 45 (2014) 653–662.
[5] L. Aresti, P. Christodoulides, G. Florides, A review of the design aspects of ground heat exchangers, Renew. Sustain. Energy Rev. 92 (2018) 757–773.
[6] S. Barbi, F. Barbieri, S. Marinelli, B. Rimini, S. Merchiori, B. Larwa, M. Bottarelli, M. Montorsi, Phase change material-sand mixtures for distributed latent heat thermal energy storage: interaction and performance analysis, Renew. Energy 169 (2021) 1066–1076.
[7] H. Yang, P. Cui, Z.H. Fang, Vertical borehole ground source heat pumps: a review of models and systems, Appl. Energy 87 (2010) 16–27.
[8] T. You, W. Wu, W. Shi, B. Wang, X. Li, An overview of the problems and solutions of soil thermal imbalance of ground-coupled heat pumps in cold regions, Appl. Energy 177 (2016) 515–536.
[9] K. Allaerts, M. Coomans, R. Salenbien, Hybrid ground-source heat pump system with active air source generation, Energy Convers. Manag. 90 (2015) 230–237.
[10] J. M Corberán, A. Cazorla-Marín, J. Marchante-Avellaneda, C. Montagud, Dual source heat pump, a high efficiency and cost-effective alternative for heating, cooling and DHW production, Int. J. Low Carbon Technol. 13 (2018) 161–176.
[11] M. Bortoloni, M. Bottarelli, Y. Su, A study on the effect of ground surface boundary conditions in modelling shallow ground heat exchangers, Appl. Therm. Eng. 111 (2017) 1371–1377.
[12] M. Bottarelli, Testing of a dual-source heat pump coupled with flat-panel ground heat exchangers, Int. J. Low Carbon Technol. 14 (2019) 247–255.
[13] V. Somogyi, V. Sebestyén, G. Nagy, Scientific achievements and regulation of shallow geothermal systems in six European countries – a review, Renew. Sustain. Energy Rev. 68 (2017) 934–952.
[14] M. Habibi, A. Hakkaki-Fard, Evaluation and improvement of the thermal performance of different types of horizontal ground heat exchangers based on techno-economic analysis, Energy Convers. Manag. 171 (2018) 1177–1192.
[15] M. Bottarelli, F.J. González Gallero, Energy analysis of a dual-source heat pump coupled with Phase Change Materials, Energies 13 (2020) 2933.
[16] M. Bottarelli, L. Gabrielli, Financial and economic analysis for ground coupled heat pump using shallow ground heat exchangers, Sustain. Cities Soc. 20 (2016) 71–80.
[17] M. Bottarelli, M. Bortoloni, Y. Su, On the sizing of a novel Flat-Panel ground heat exchanger in coupling with a dual-source heat pump, Renew. Energy 142 (2019) 552–560.
[18] C. Han, X. Yu, Sensitivity analysis of a vertical geothermal heat pump system, Appl. Energy 170 (2016) 148–160.
[19] W. Zhao, Z. Hu, W. He, S. Zhang, H. Yu, G. Xu, H. Chen, Intermittent mode analysis of a borehole ground heat exchanger with novel phase change backfill materials, Appl. Therm. Eng. 189 (2021) 116716.
[20] L. Liu, G. Cai, X. Liu, S. Liu, A.J. Puppala, Evaluation of thermal-mechanical properties of quartz sand–bentonite–carbon fiber mixtures as the borehole backfilling material in ground source heat pump, Energy Build. 202 (2019) 109407.
[21] R. Stropnik, R. Koželj, E. Zavrl, U. Stritih, Improved thermal energy storage for nearly zero energy buildings with PCM integration, Sol. Energy 190 (2019) 420–426.
[22] P.K.S. Rathore, S.K. Shukla, Potential of macroencapsulated pcm for thermal energy storage in buildings: a comprehensive review, Construct. Build. Mater. 225 (2019) 723–744.
[23] W. Yang, R. Xu, B. Yang, J. Yang, Experimental and numerical investigations on the thermal performance of a borehole ground heat exchanger with PCM backfill, Energy 174 (2019) 216–235.
[24] F. Chen, J. Mao, C. Li, P. Hou, Y. Li, Z. Xing, S. Chen, Restoration performance and operation characteristics of a vertical U-tube ground source heat pump system with phase change grouts under different running modes, Appl. Therm. Eng. 141 (2018) 467–482.
[25] D. Qi, L. Pu, F. Sun, Y. Li, Numerical investigation on thermal performance of ground heat exchangers using phase change materials as grout for ground source heat pump system, Appl. Therm. Eng. 106 (2016) 1023–1032.
[26] Z. Khan, Z. Khan, A. Ghafoor, A review of performance enhancement of PCM based latent heat storage system within the context of materials, thermal stability and compatibility, Energy Convers. Manag. 115 (2016) 132–158.
[27] A. Sharma, V.V. Tyagi, C.R. Chen, D. Buddhi, Review on thermal energy storage with phase change materials and applications, Renew. Sustain. Energy Rev. 13 (2009) 318–345.
[28] H. Akeiber, P. Nejat, M.Z.A. Majid, M.A. Wahid, F. Jomehzadeh, I. Zeynali Famileh, J.K. Calautit, B.R. Hughes, S.A. Zaki, A review on phase change material (PCM) for sustainable passive cooling in building envelopes, Renew. Sustain. Energy Rev. 60 (2016) 1470–1497.
[29] R.K. Sharma, P. Ganesan, V.V. Tyagi, H.S.C. Metselaar, S.C. Sandaran, Developments in organic solid-liquid phase change materials and their applications in thermal energy storage, Energy Convers. Manag. 95 (2015) 193–228.
[30] F. Kleiner, K. Posern, A. Osburg, Thermal conductivity of selected salt hydrates for thermochemical solar heat storage applications measured by the light

flash method, Appl. Therm. Eng. 113 (2017) 1189–1193.
[31] M.F. Junaid, Z.u. Rehman, M. Čekon, J. Čurpek, R. Farooq, H. Cui, I. Khan, Inorganic phase change materials in thermal energy storage: a review on perspectives and technological advances in building applications, Energy Build. 252 (2021) 111443.
[32] Y. Rabin, E. Korin, Incorporation of phase-change materials into a ground thermal energy storage system: theoretical study, J. Energy Resour. Technol. 118 (1996) 237–241.
[33] H. Lei, N. Zhu, Analysis of phase change materials (PCMs) used for borehole fill materials, Trans. Geoth. Resour. Counc. 33 (2009) 93–98.
[34] X. Li, C. Tong, L. Duanmu, L. Liu, Research on U-tube heat exchanger with shape-stabilized phase change backfill material, Procedia Eng. 146 (2016) 640–647.
[35] F. Chen, J. Mao, S. Chen, C. Li, P. Hou, L. Liao, Efficiency analysis of utilizing phase change materials as grout for a vertical U-tube heat exchanger coupled ground source heat pump system, Appl. Therm. Eng. 130 (2018) 698–709.
[36] P. Eslami Nejad, M. Bernier, A preliminary assessment on the use of phase change materials around geothermal boreholes, Build. Eng. 119 (2) (2013) 312–321.
[37] J.L. Wang, J. De Zhao, N. Liu, Numerical simulation of borehole heat transfer with phase change material as grout, Appl. Mech. Mater. 577 (2014) 44–47.
[38] M. Zhang, X. Liu, K. Biswas, J. Warner, A three-dimensional numerical investigation of a novel shallow bore ground heat exchanger integrated with phase change material, Appl. Therm. Eng. 162 (2019) 114297.
[39] P.K. Dehdezi, M.R. Hall, A.R. Dawson, Enhancement of soil thermo-physical properties using microencapsulated Phase Change Materials for ground source heat pump applications, Appl. Mech. Mater. 110–116 (2011) 1191–1198.
[40] M. Bottarelli, M. Bortoloni, Y. Su, Heat transfer analysis of underground thermal energy storage in shallow trenches filled with encapsulated phase change materials, Appl. Therm. Eng. 90 (2015) 1044–1051.
[41] M. Bottarelli, M. Bortoloni, Y. Su, C. Yousif, A.A. Aydin, A. Georgiev, Numerical analysis of a novel ground heat exchanger coupled with phase change materials, Appl. Therm. Eng. 88 (2015) 369–375.
[42] IDEAS – Novel building Integration Designs for increased Efficiencies in Advanced Climatically Tunable Renewable Energy Systems. https://www.horizon2020ideas.eu [Accessed 9th February 2022].
[43] CLIWAX – Materiali a cambio di fase per l'harvesting energetico in climatizzazione. http://cliwax.it [Accessed 9th February 2022].
[44] PCM Products Ltd., https://www.pcmproducts.net [Accessed 9th February 2022].
[45] Rigid Stem Resistance Thermometers - Type 16, https://www.tc.co.uk/downloads/Rigid-Stem-Resistance-Thermometers-Type-16.pdf [Accessed 11st May 2021].
[46] Delta strumenti, thermocouple wire (in Italian), https://www.deltastrumenti.it/images/pdf/termocoppie/in_cavetto/Termocoppia_cavetto.pdf [Accessed 9th February 2022].
[47] TT - Digital multipoint temperature probe, https://www.sgm-lektra.com/product/tt-2/[Accessed 11st May 2021].
[48] HFP01 heat flux sensor, https://www.hukseflux.com/products/heat-flux-sensors/heat-flux-meters/hfp01-heat-flux-sensor [Accessed 9th February 2022].
[49] Belimo flow meter, https://www.belimo.com/it/shop/en_GB/Sensori/Sonde-da-tubazione-%28acqua%29/FM025R-SZ/p?code=FM025R-SZ [Accessed 9th February 2022].
[50] DT85 Series 4 Data Logger, https://assets.thermofisher.com/TFS-Assets/ANZ/brochures/datataker-dt85-series-4-data-logger.pdf [Accessed 9th February 2022].
[51] MICROCLIMA U - Ultrasonic compact thermal energy meter, https://www.maddalena.it/en/products/thermal-energy/microclima-u/95 [Accessed 9th February 2022].
[52] CMe3000, https://www.elvaco.se/en/product/infrastructure1/cme3000-m-bus-gateway-for-fixed-network–1050015 [Accessed 9th February 2022].
[53] Weather station Vantage Pro2, https://www.davisinstruments.com/vantage-pro2/[Accessed 11st May 2021].
[54] SR20 PYRANOMETER, https://www.hukseflux.com/products/solar-radiation-sensors/pyranometers/sr20-pyranometer [Accessed 9th February 2022].